



Plasticization and crosslinking effects of acetone–formaldehyde and tannin resins on wheat protein-based natural polymers

Xiaoqing Zhang*, My Dieu Do

CSIRO Materials Science and Engineering, Private Bag 33, Clayton South MDC, Clayton South, VIC 3169, Australia

ARTICLE INFO

Article history:

Received 26 February 2009

Received in revised form 30 March 2009

Accepted 31 March 2009

Available online 5 April 2009

Keywords:

Wheat proteins

Acetone–formaldehyde and tannin resins

Plasticization

Crosslinked network

Mechanical performance

ABSTRACT

Efficient plasticization and sufficient crosslinking were achieved by using an acetone–formaldehyde (AF) resin as an additive in the thermal processing of wheat protein-based natural polymers. The mobile AF resin and its strong intermolecular interactions with a wheat protein matrix produced sufficient flexibility for the plastics, while the covalent bonds formed between AF and the protein chains also caused the water-soluble resin to be retained in the materials under wet conditions. The mechanical properties of the materials were also enhanced as an additional benefit due to the formation of crosslinked networks through the polymer matrix. Tensile strength was further enhanced when using AF in conjunction with tannin resin (AFTR) in the systems as rigid aromatic structures were formed in the crosslinking segments. Different components in wheat proteins (WPs) or wheat gluten (WG) (e.g., proteins, residual starch and lipids) displayed different capabilities in interaction and reaction with the AFTR additives, and thus resulted in different performances when the ratio of these components varied in the materials. The application of the AFTR additives provides a feasible methodology to thermally process wheat protein-based natural polymers with improved mechanical performance and water-resistant properties.

© 2009 Elsevier Ltd. All rights reserved.

1. Introduction

Development of polymer materials from agricultural products-based natural polymers has become an important pathway to produce sustainable materials for various applications. Considerable attention has been focused on natural polymer wheat proteins in recent years due to their excellent properties, renewable and biodegradable capabilities and low price among plant proteins. However, one of the biggest challenges is to thermally process wheat protein-based materials with sufficient mechanical properties, especially when exposed to wet conditions. The existence of strong self-association among protein segments through intra- and intermolecular interactions requires a large amount of plasticizers in the thermal processing to reduce those strong interactions, increase the mobility of the protein chains, and therefore to improve the flexibility and the extensibility of the materials.^{1–8} Water is the most ubiquitous plasticizer because of its strong capability to modify the mobility of the protein molecules. Natural wheat proteins contain around 8–13% of moisture, which is difficult to remove completely from the system. Thus water always exists in the materials at some level regardless of using any other plasticizers. Glycerol is the other common plasticizing agent having a high retention in protein material due to its high boiling point and strong hydro-

gen bonding with proteins.^{3,4,8–12} Other plasticizers such as polyols, fatty acids and amines have also been examined for wheat protein systems.^{13–15} However, the use of these plasticizers significantly reduces the material strength, especially the water-resistant strength. In addition, most of these plasticizers are difficult to be retained in the materials under wet conditions since the hydrogen bonding interactions between these plasticizers and the protein matrix are easily destroyed when exposed to water.

Formation of a crosslinked network is a common way to build up additional covalent linkages within the protein matrix to enhance the mechanical strength and water-resistant properties. Aldehyde crosslinkers are the most effective crosslinkers, and have been widely used in many protein-based materials such as wheat gluten,^{16–18} sunflower or soy proteins,^{19–22} collagen,²³ corn zein,²⁴ whey or cottonseed proteins,^{25–27} and wool fibres^{28,29} to promote the formation of crosslinked networks. Other crosslinkers such as carbodiimides,^{30,31} epoxy compounds or genipin^{32,33} have also been studied for protein systems. Recently, alkoxysilanes were applied as crosslinking agents to enhance the mechanical properties of wheat gluten.³⁴ Chemical modification of wheat proteins through grafting mobile polymer segments onto the protein materials and then applying another crosslinker in the system to conduct coupling reactions has also been demonstrated to be an efficient way to achieve effective crosslinking through the whole protein matrix.^{35,36} This methodology also provides a pathway to introduce designed functional groups into the materials for

* Corresponding author. Tel.: +61 3 95452653; fax: +61 3 95441128.
E-mail address: Xiaoqing.Zhang@csiro.au (X. Zhang).

developing biomaterial from natural polymers. Certainly such chemical modifications need to be conducted before the thermal processing.

It is desirable to use a single additive in the thermal processing which can act as both plasticizer and crosslinker in wheat protein systems to achieve sufficient flexibility and extensibility of protein matrix, while the reactive groups in the additive can also react with the proteins to form covalent bonds with the polymer matrix. Such chemical linkages would cause the additives to be retained in the systems even under wet or high humidity conditions. In this work, a water-soluble acetone–formaldehyde (AF) resin in conjunction with natural tannin resin was applied to wheat proteins in thermal processing. The free formaldehyde content in this AF resin was reduced to below 0.1% via a combination of hydrogen peroxide and urea treatment,³⁷ which allowed the resin to meet the requirement in a wide range of packaging products. Currently these resins are used as water-resistant additives in paperboard manufacturing by packaging industries to replace formaldehyde- or paraformaldehyde-based resins.³⁸ With structures similar to polyols, the mobile AF molecules should act as an efficient plasticizer for wheat proteins. The methylation structures of AF should undergo further condensation reactions to form crosslinked networks with a series of functional groups in wheat proteins. The relatively low reactivity (as compared to other aldehyde-based crosslinkers) of the AF resin would only make it possible to build chemical linkages between the AF molecules and the protein matrix under usual thermal processing conditions, but would not produce a polymer network with a high crosslink density, which could greatly reduce the plasticization effect. On the other hand, tannin as a natural polyphenolic product derived from plants has a long history as anti-oxidant additives applied in food processing, or as a modifier in leather fabrication. On many occasions this has been used as a natural product to replace phenolic chemicals with similar chemistry in crosslinking reactions.^{39–42} When using a combination of AF and a tannin resin (AFTR) in the system, the tannin could react with both the AF and the amino and/or hydroxy functional groups of wheat proteins through a condensation mechanism under thermal processing conditions, and then form crosslinked networks among all components through the whole materials. New functional properties could also be introduced to the materials.

Two kinds of raw wheat proteins were used in the study, and all materials were thermally processed under a natural pH of the mixtures of all components (pH 6.0–6.5) to avoid high reactivity among AFTR and WP or WG at either high or low pH. These pH conditions are also desirable for edible packaging products.^{43–46} The ratio of AF and tannin was varied, and the mechanical properties of the processed materials were measured after condition-

ing the samples under standard relative humidity (RH = 50%). Dynamic mechanical analysis (DMA) and high-resolution solid-state NMR spectroscopy were also conducted to examine the glass transition temperatures, material modulus, glass transition, chemical structures and molecular motions of the materials. The reactions/interactions between the additives and each component in the wheat protein materials were also studied to understand the material performance.

2. Experimental

2.1. Materials

Vital wheat gluten (WG) and deamidated wheat protein (WP) were supplied by Manildra Group Australia. WG contained 80% proteins, 15% residual starch, 4% lipid, and around 1% fibres and other impurities on dry basis, while WP contained over 90% protein, 5% lipid and a small amount of residual starch (3%) with other minor impurities. The deamidation was conducted under mild conditions, resulting in 30–35% of the –CONH in the side chains being broken, leaving –COOH as the end groups. The moisture content of both WG and WP was ~12 wt % as received. Acetone–formaldehyde (AF) resin (ULTRA-GUARD™, 50 wt % in water) was obtained from National Starch & Chemical Company. Colatan tannin was produced by hydrolysis of Argentine Quebracho extract and was supplied by Manildra Group Australia. The tannin content was 95%, while the moisture content was 5%. All of these raw materials were used as received without further treatment or purification.

Each sample with a designated formulation (listed in Table 1 as data before compression moulding) was mixed with a high-speed mixer for 1 min at a speed of 3000 rpm, left overnight, and then compression moulded at an optimum temperature of 130 °C for 5 min under a pressure of 12 tons. The sample size was 145 mm × 145 mm with a thickness of 1.0 ± 0.1 mm. WP and WG powder samples with natural moisture content were also compression moulded under the same conditions (referred to as WP-0 and WG-0), and the sample size was of 45 mm × 10 mm with a thickness of 1.0 ± 0.1 mm to avoid sample cutting for DMA testing as the samples were too brittle to be cut. After conditioning these thermally processed samples for one week at room temperature (23 °C) under relative humidity (RH) of 50%, a measure of the moisture content in each sample was determined by the weight loss measured after drying the samples at 105 °C for 6 h. All WG and WP samples contained 10–11 wt % of moisture after the conditioning. The resin content in these samples was calculated assuming no resin loss in the processing and conditioning. Both resin and moisture contents in the samples after compression moulding and conditioning are also listed in Table 1.

Table 1
Compositions (wt parts or wt %) of WP or WG materials before and after compression moulding

Samples	Before compression moulding							After compression moulding and conditioning at RH = 50% for 7 days (wt %)	
	WP or WG (wt parts)		AFTR (wt parts)			Overall content (wt %)		H ₂ O	Resin
	Solids	H ₂ O	AF	H ₂ O	Tannin	H ₂ O	Resin		
WP-A1	100	13.6	8.8	8.8	0	17.1	6.7	10.7	7.2
WP-A2	100	13.6	13.4	13.4	0	19.2	9.5	10.9	10.5
WP-A3	100	13.6	18.3	18.3	0	21.3	12.2	10.3	13.7
WP-B1	100	13.6	12.1	13.4	1.3	19.2	9.5	11.1	10.5
WP-B2	100	13.6	10.8	13.4	2.6	19.2	9.5	10.4	10.6
WP-B3	100	13.6	9.4	13.4	4.0	19.2	9.5	11.2	10.5
WG-A1	100	13.6	8.8	8.8	0	17.1	6.7	10.2	7.3
WG-A2	100	13.6	13.4	13.4	0	19.2	9.5	11.1	10.5
WG-A3	100	13.6	18.3	18.3	0	21.3	12.2	10.7	13.8
WG-B1	100	13.6	12.1	13.4	1.3	19.2	9.5	10.7	10.5
WG-B2	100	13.6	10.8	13.4	2.6	19.2	9.5	10.0	10.6
WG-B3	100	13.6	9.4	13.4	4.0	19.2	9.5	11.0	10.5

Water uptake and solubility tests of the samples were conducted by soaking the samples (after the conditioning) in distilled water (1 wt part of sample in ~50 wt parts of water) for 7 h under sonication using a Branson B-3200 sonicator. Water uptake and solubility data were measured by weighing the wet samples after carefully removing water on the sample surface, weighing the samples again after drying the wet samples at 105 °C for 6 h and comparing with the data of the samples after conditioning.

2.2. Instrumentation

All sample characterizations were conducted after conditioning under RH = 50% for 7 days at room temperature. Mechanical properties were determined on an INSTRON 5566P with a cross-head speed of 50 mm/min. The data for each sample were obtained from an average of testing seven dog-bone specimens with an effective length of 30 mm and width of 6 mm. DMA experiments were conducted on a Perkin-Elmer PYRIS™ Diamond DMA in dual cantilevers bending mode at a frequency of 1 Hz. The temperature range was set at –100 °C to 140 °C, and the heating rate was 2 °C/min. The storage modulus (E'), the loss modulus (E'') and $\tan \delta$ were recorded as a function of temperature throughout the experiment.

High-resolution solid-state NMR experiments were conducted at room temperature using a Varian Unity plus spectrometer at resonance frequencies of 75 MHz for ^{13}C and 300 MHz for ^1H . ^{13}C NMR spectra were observed under either cross-polarization, magic angle spinning and high power dipolar decoupling (CP/MAS/DD) technique, or using a single 90° pulse excitation (SPE) method under MAS and DD conditions. The 90° pulse was 6 μs for H-1 and C-13, while the spinning rate of MAS was set at a value around 6 kHz. A contact time of 1.0 ms was used for measuring CP/MAS spectra, while the repetition time was 2 s for both CP/MAS and SPE/MAS measurements. The chemical shift of ^{13}C CP/MAS spectra was

determined by taking the carbonyl carbon of solid glycine (176.03 ppm) as an external reference standard. ^1H spin-lattice (T_1) data were measured through the change of ^{13}C magnetization prepared by CP after the inversion–recovery pulse sequence in the ^1H channel. ^1H MAS NMR spectra were obtained with the same MAS rate, and TMS was used as an external chemical shift reference. ^1H spin–spin (T_2) relaxation times were measured through the decay of ^1H intensities in MAS spectra observed by the CPMG (t_1 of 40 μs) pulse sequence with a repetition time of 2 s and a 90° pulse length of 2.5 μs . The T_2 values were obtained from fitting the intensities of resonances and no spectral de-convolution was applied. These methods were described in our previous publications.^{8,12,18,34,36} ^{13}C solution NMR spectra for the water-soluble additives and water-soluble components of the WP or WG materials were measured using the same spectrometer with a 10-mm solution probe head.

3. Results and discussion

3.1. Interactions between AFTR additives and WP or WG

Both AF resin and Colatan tannin are water-soluble resins, and most of their ^{13}C resonances are not overlapping to each other. Figure 1 shows the ^{13}C solution NMR spectra of the AF and the mixture of AFTR in water solution. For the AF resin, the $-\text{CH}_2\text{OH}$ (63 ppm) is predominant in the spectrum in conjunction with the $>\text{C}=\text{O}$ (219 ppm), $-\text{CH}_2\text{OCH}_2-$ (72 ppm), $-\text{CH}_3$ (30 ppm) and other resonances formed in condensation reactions of acetone and formaldehyde. The signals at 165–174 ppm are due to $-\text{COOH}$ and ester/amide species derived from the treatment using hydrogen peroxide and urea to react with the residual formaldehyde. The Colatan tannin resonances at a range of 60–110 ppm of the AFTR spectrum are due to the anhydroglu-

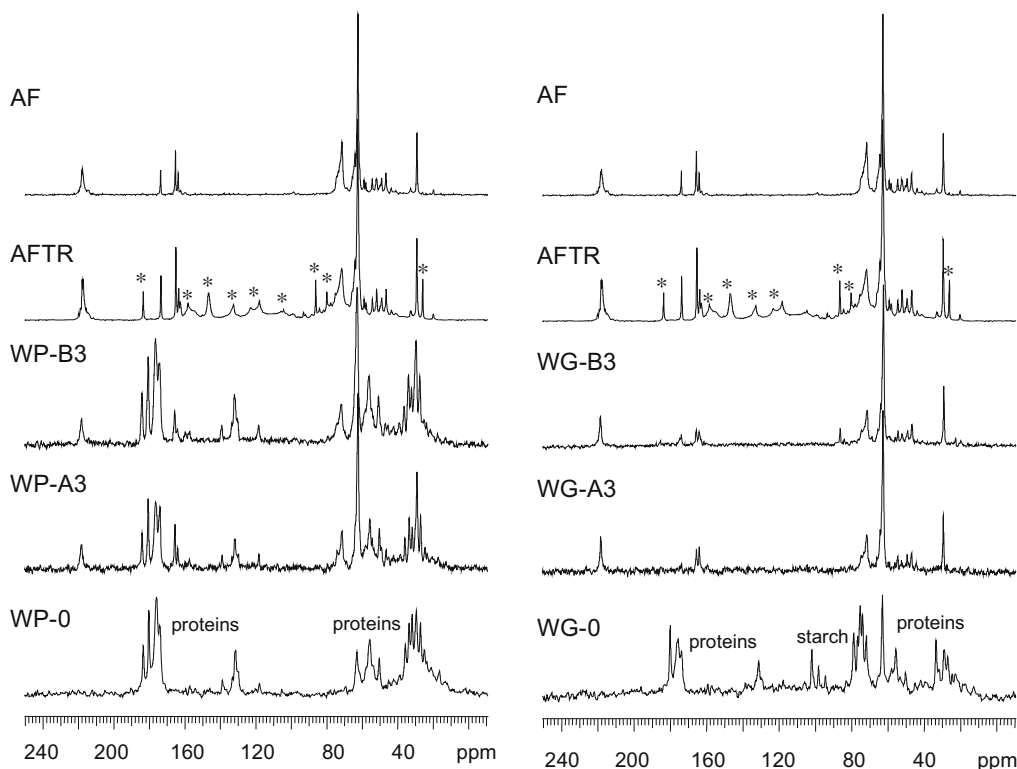


Figure 1. ^{13}C solution NMR spectra of AF, AFTR resins, and those of the soluble parts of WP or WG samples obtained after sonication for 7 h in water. The “*” peaks in the spectra of AFTR are due to the resonances of Colatan tannin in the AFTR mixture.

Table 2

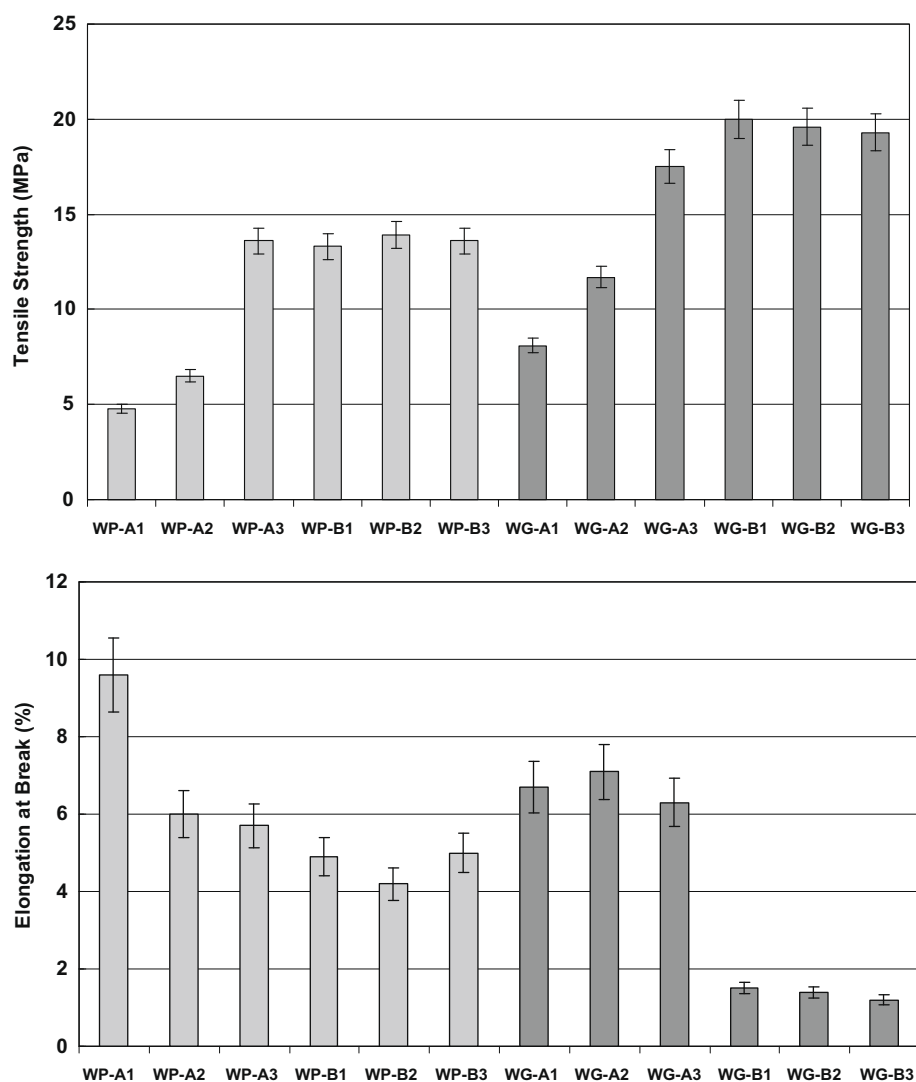
Water uptake and solubility (wt %) for WP or WG materials after sonication

Samples	Water uptake (%)	Solubility (%)
WP-0	456	26.9
WP-A1	397	12.7
WP-A2	391	11.5
WP-A3	379	11.0
WP-B1	406	10.4
WP-B2	398	9.0
WP-B3	370	10.2
WG-0	95.8	15.5
WG-A1	74.5	4.7
WG-A2	85.2	2.2
WG-A3	77.8	3.6
WG-B1	76.7	1.1
WG-B2	72.2	3.6
WG-B3	68.1	3.1

case unit, while those at 110–160 ppm are assigned to the phenolic structures of the tannin.

When applying either AF or AFTR to WP or WG materials during thermal processing, a large proportion of these water-soluble resins were entrapped in the polymer matrix as demonstrated in the solubility data listed in Table 2. Sonication was applied to accelerate the extraction to remove the soluble parts from the WP or WG materials into the water phase. As many unstable chem-

ical bonds formed between AF and WP or WG and even those in WP or WG matrix could be disrupted during the sonication, the solubility of these materials obtained should be higher than those under normal wet application conditions. The solubility for the WP- or WG-only sample after thermal processing (WP-0 or WG-0) was 26.9% or 15.5% after sonication for 7 h in water. These data were significantly reduced from 100% for the WP powder or 35% for the WG powder under the same conditions, which is attributed to the thermal crosslinking in the WP or WG matrix that occurred under the compression moulding conditions. When 7–14% water-soluble resins AF or AFTR were introduced into WP or WG systems, the solubility was further reduced, especially in WG materials; only a minimal amount of weight loss (1–5%) was observed for WG-A or -B samples after sonication (Table 2). The solubility for WP materials containing AF or AFTR (WP-A and -B materials) was reduced to 9–13%. These results indicate that covalent bonds were indeed formed between AF or AFTR and WG or WP, which resulted in formation of crosslinked networks in these materials. The water uptake data for both WP and WG samples containing AF or AFTR were also reduced as compared to those for WP-0 or WG-0, but the change was not very significant. This could be due to the relatively low crosslink density formed in these materials plus the hydrophilic nature of both the protein matrix and the cross-linking segments derived from AF or AFTR.

**Figure 2.** Mechanical properties (tensile strength and elongation at break) of WP and WG materials.

The solution ^{13}C NMR spectra of the soluble components (obtained after sonication) for either WP or WG samples displayed similar characteristics, and the typical spectra (-A3 and -B3) are shown in Figure 1 to compare with the soluble parts of WP-0, WG-0, and those of the original soluble AF and AFTR. For WP-0 or WG-0, the soluble components consisted of proteins or proteins and starch as detected by the NMR spectra. However, only AF signals were observed in WG-A or -B samples (see WG-A3 and -B3 as examples) in the soluble phase, while both WG and tannin components remained insoluble after the sonication. This indicates that the small amount (1–5%) of soluble components in WG materials was only due to free AF species. For WP-A and -B samples, both WP and AF signals existed in the soluble components, but no signal of the tannin resin was detected in the soluble phase of WP-B3. Although it is difficult to determine the ratio of AF and WP in the soluble phase, the overall solubility (9–13%) was significantly reduced as compared to 26.9% in the WP-0 plus 7–14% soluble resins applied. In both WP and WG systems, the resonances of Colatan tannin were not observed in the soluble phase, indicating its sufficient reactivity with AF and WP/WG in the system under the compression moulding conditions. However, the addition of tannin resin did not generate further reduction in solubility and water uptake data for either the WP or WG materials, suggesting no additional crosslinking density was produced.

3.2. Mechanical properties of the WP and WG materials

A significant plasticization effect was produced when using either AF or AFTR as additives in both WP and WG materials. The compression-moulded samples displayed sufficient flexibility after the conditioning under RH = 50%, and it became possible to cut the samples for mechanical testing. In contrast, the WP-0 and WG-0 samples were too brittle to handle for conducting tensile testing under the same conditions.

Figure 2 shows the results of tensile strength and elongation at break for WP or WG materials after the conditioning at RH = 50%. The moisture contents of all of the samples were quite similar, around 10–11% as shown in Table 1. When the amount of AF resin increased in the WP-A samples, the tensile strength was increased from 4.8 to 13.6 MPa, while the elongation at break was reduced from 9.6% to 5.7%. These results indicate a crosslinking effect in the materials besides the plasticization. The increase in the amount of AF enhanced the crosslinking effect, resulting in an increase in the tensile strength and a reduction of elongation of the materials. When keeping the total amount of resin constant at a level of 10.5% (WP-A2), while increasing the amount of tannin in the resins to replace a proportion of AF (WP-B samples), the tensile strength was enhanced over 100% as compared to that of WP-A2, while the elongation was reduced to 4–5%. This result should be attributed to the formation of crosslinking segments involving rigid aro-

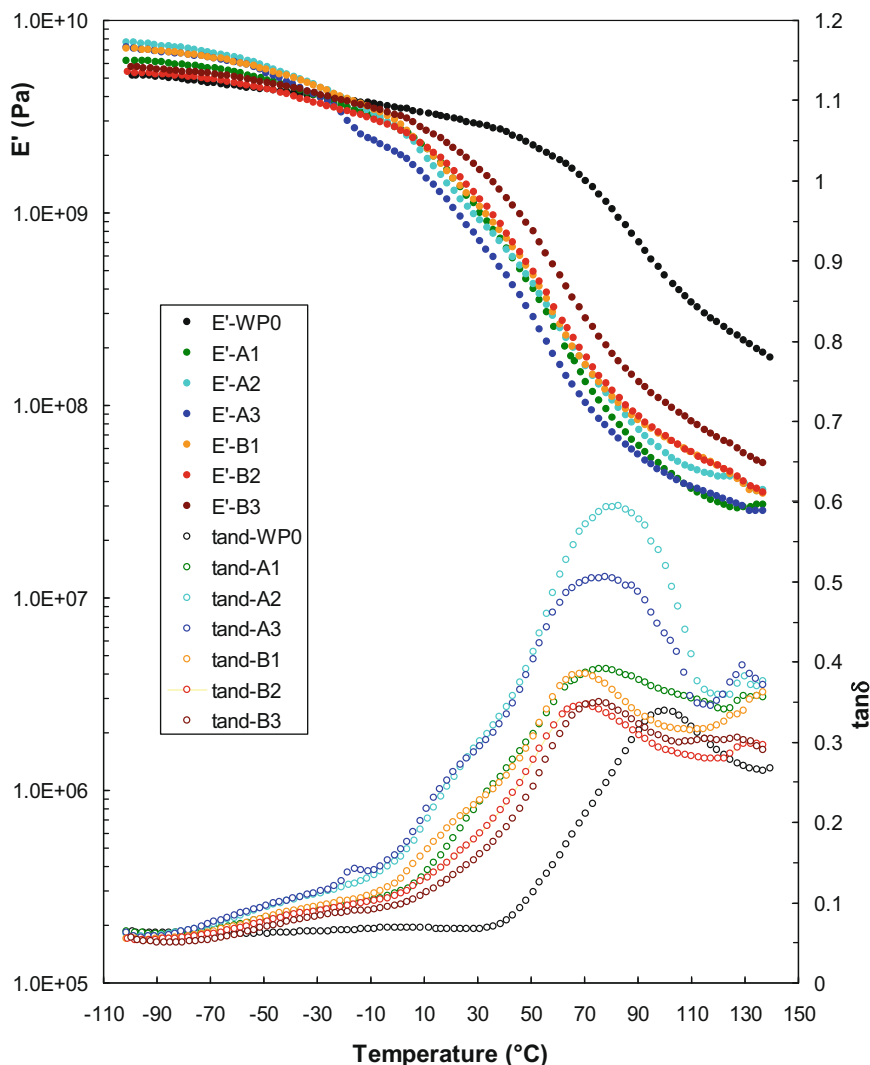


Figure 3. DMA data (E' and $\tan \delta$) of WP materials.

matic structures (tannin) in the materials rather than only having the mobile aliphatic segments derived from AF resin. The amount of Colatan tannin was not further increased in the materials as it would further reduce the flexibility of the materials and would cause material handling difficulties at RH = 50%.

The usage of AF or AFTR additives in the WG system resulted in a tensile strength stronger than that of the WP systems (Fig. 2). Addition of tannin resin further enhanced the tensile strength (reaching to 19.5–20 MPa for WG-B samples), and the material elongation was reduced to around 1.5%. Note that the moisture content of the WG samples was still around the same level (10–11%) as that for the WP sample after conditioning at RH = 50%. This result suggests that the additives might behave differently in WG and WP materials.

DMA was conducted for the thermally processed WP and WG materials after the conditioning with results shown in Figures 3 and 4. The data for WP-0 or WG-0 were also displayed for comparison. The E' and $\tan \delta$ curves of these samples were similar to other plasticized WP or WG samples reported previously.^{6–8,34–36,46} Key DMA data of these WP and WG samples are listed in Table 3. The temperature when glass transition started ($T_{g-start}$) was taken from the onset of E' decrease with increasing temperature. The $T_{g-start}$ for WP-0 or WG-0 occurred at 51 or 58 °C. It was decreased significantly when AF or AFTR was used in both WP and WG materials, and in many cases the $T_{g-start}$ was below room temperature, sug-

gesting a significant plasticization effect on the materials. Consequently, the E' for the materials containing AF or AFTR at room temperature (25 °C) was decreased correspondingly as compared to that of WP-0 or WG-0. The $T_{g-start}$ occurred at 11–14 °C for WP-A samples, while the $\tan \delta$ peak corresponding to the T_g transitions shifted to 68–83 °C (compared to 100 °C for WP-0). The usage of tannin did increase both the $T_{g-start}$ of WP-B samples and their E' at room temperature as compared to those of WP-A2. The $\tan \delta$ peaks corresponding to T_g transitions of WP materials were all very broad. However, the maximum values of $\tan \delta$ increased from 0.34 for WP-0 to 0.39 for WP-A1, then to over 0.50 for WP-A2 and -A3 samples. Such mobility enhancement at the T_g transition indicates that the crosslinking segments derived from AF were relatively long and mobile, and the crosslink density was low. When AFTR was used in the WP system (WP-B), the $\tan \delta$ maximum was around 0.35–0.39, at a level similar to that of WP-0. Such motional restriction at the T_g transition should be attributed to the formation of crosslinking segments containing rigid tannin aromatic structures. The multi-functionality of tannin could form crosslinking structures with AF segments, and the mobility of the crosslinking segments would be reduced.

The situation of the WG materials was different from that of the WP samples. The values of $T_{g-start}$ for most WG samples were lower than those in the WP materials, especially for those having AFTR in the systems. When AFTR was used in the WG materials, the $T_{g-start}$

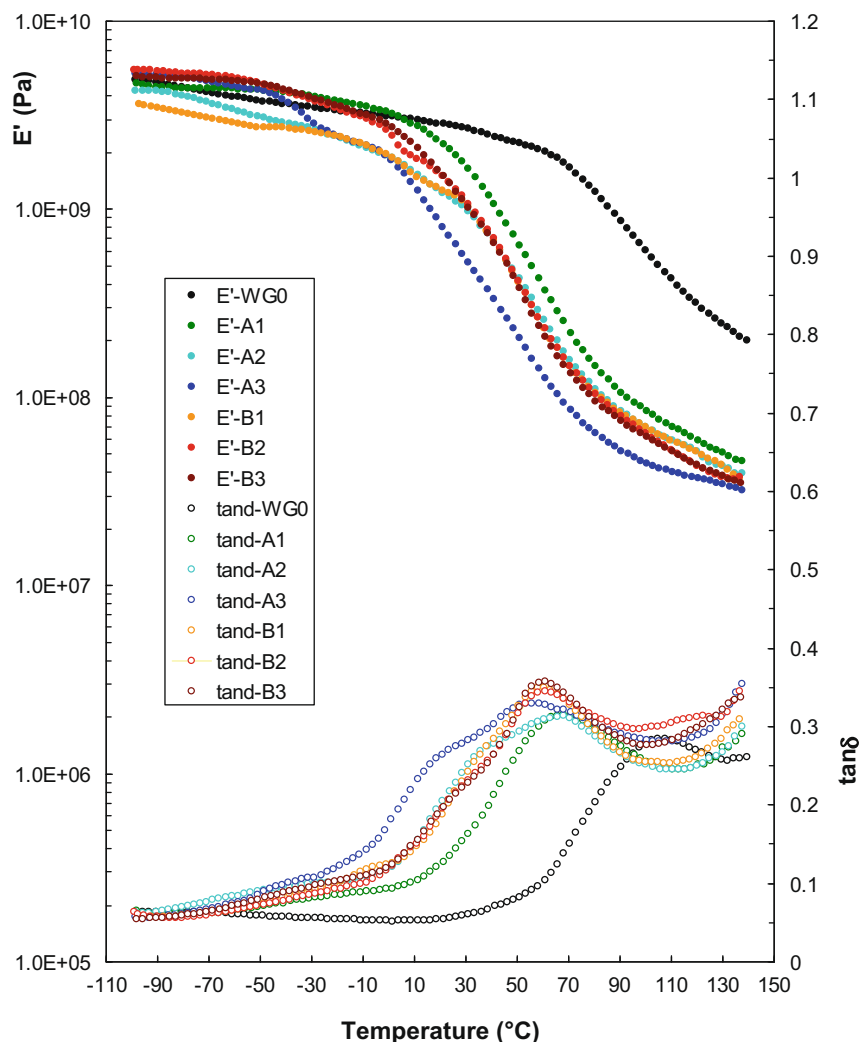


Figure 4. DMA data (E' and $\tan \delta$) of WG materials.

Table 3

Key DMA data of WP or WG materials

Samples	$T_{g-start}$ (°C)	E' at 25 °C (GPa)	$\tan \delta - \alpha$ (°C)	$\tan \delta$ max
WP-0	51	3.01	100	0.34
WP-A1	11	2.08	75	0.39
WP-A2	14	1.16	83	0.59
WP-A3 ^a	14	0.72	78	0.51
WP-B1	16	1.23	68	0.39
WP-B2	19	1.29	71	0.35
WP-B3	24	1.37	76	0.35
WG-0	58	2.78	107	0.25
WG-A1	18	1.35	80	0.32
WG-A2	11	1.17	68	0.32
WG-A3 ^a	0.4	0.87	56	0.33
WG-B1	4.8	1.38	61	0.35
WG-B2	6.1	1.53	61	0.34
WG-B3	2.8	2.06	61	0.36

^a WP-A3: $\tan \delta - \beta$ at -16 °C (peak maximum 0.142); WG-A3: $\tan \delta - \beta$ at -31 °C (peak maximum 0.111).

and the $\tan \delta$ of T_g transition for WG-B samples were in the range between those of WG-A2 and -A3, while their E' at 25 °C was higher than that of WG-A2 and -A3. The $\tan \delta$ maximum at T_g for WG-A or -B samples was only slightly higher than that of WP-0, and there was no significant difference between the WG-A and -B samples. The lower $T_{g-start}$ values suggest that WG experienced a plasticization effect greater than that of the WP materials, or at least some proportion of the materials did so. But $\tan \delta$ data indicate that only a small mobility enhancement at T_g was generated by using AF or AFRT in the materials. Considering the results of mechanical properties, it seemed that some proportion of the WG materials experienced a more pronounced plasticization effect, a lower $T_{g-start}$ value, but the material matrix was still rigid, which could be due

to either a weaker plasticization or a stronger crosslinking effect as compared to WP materials when using the same amount of AF or AFTR.

A minor $\tan \delta$ peak was also observed for WP-A3 or WG-A3 at -16 or -31 °C with $\tan \delta$ maximum of 0.14 and 0.11, respectively, which could be due to a T_g transition for mobile AF segments. Such transitions became distinct when the amount of AF was higher, which is similar to the cases when glycerol or other small molecules were used as plasticizers in WP or WG materials.^{6–8,34–36} However, these became too weak to be observed when the tannin resins were used in the systems, which is consistent with the reduction in the mobility of the AFTR segments.

3.3. Plasticization and crosslinking effects to each component in the materials

The main components in the WP and WG raw materials include a large number of different proteins plus residual starch and lipids as impurities. These components could interact or react differently with AF or AFTR and could show different plasticization and crosslinking effects on their molecular motions. The interactions among these components would also affect phase structures of the whole materials. An understanding of the behaviour of each component in such a complex system and the interaction among these components are fundamental in understanding the material performance and in developing materials with desired properties. Solid-state NMR spectroscopy is a useful tool to provide interaction and reactivity information in such multicomponent systems as demonstrated in our previous publications.^{4–36,46,47}

High-resolution solid-state ^{13}C NMR spectra of the WP and WG materials were measured by both CP/MAS and SPE/MAS tech-

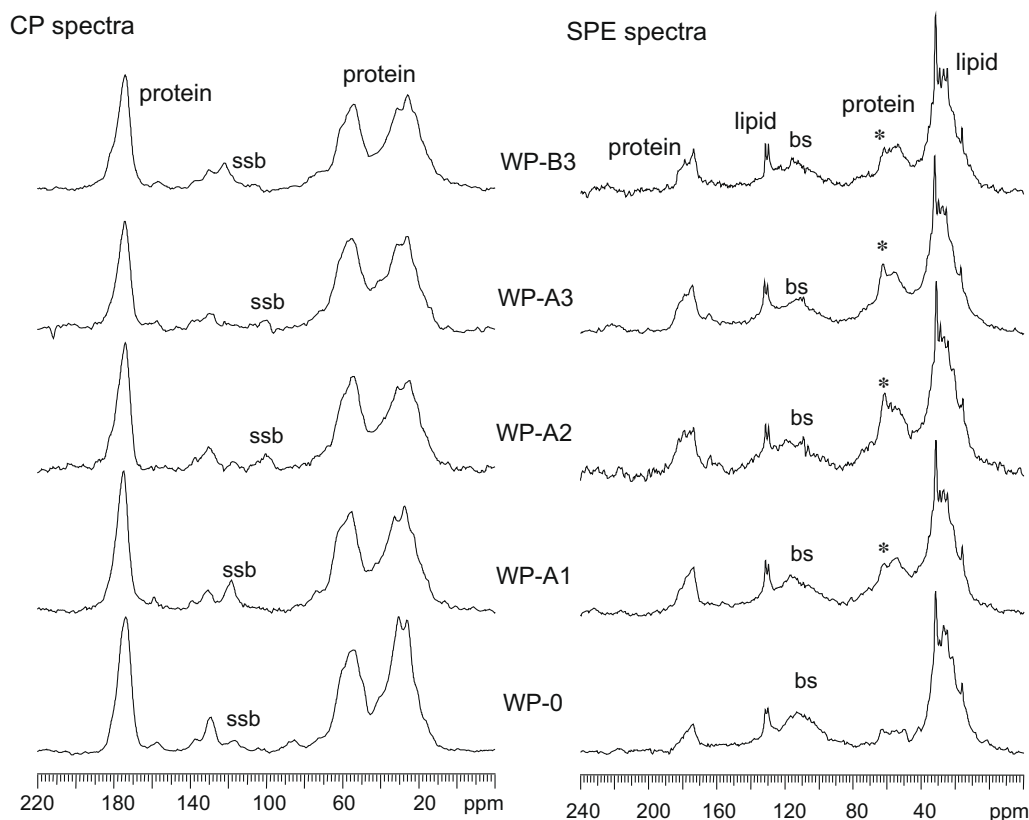


Figure 5. ^{13}C CP/MAS and SPE/MAS NMR spectra of WP materials. (ssb: spinning side band in CP/MAS spectra; bs: background signal from the spinner in SPE/MAS spectra. The peak marked with “*” is due to the signal derived from AF resin).

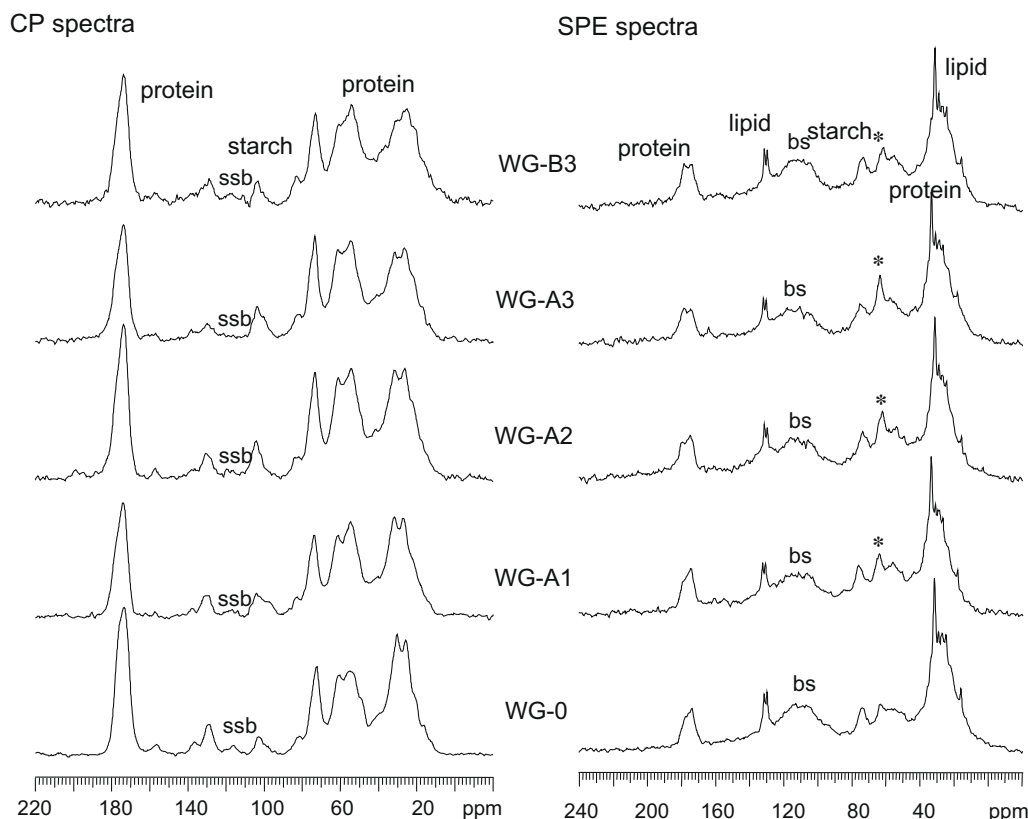


Figure 6. ^{13}C CP/MAS and SPE/MAS NMR spectra of WG materials. (ssb: spinning side band in CP/MAS spectra; bs: background signal from the spinner in SPE/MAS spectra. The peak marked with “*” is due to the signal derived from AF resin).

niques as shown in Figures 5 and 6. The CP/MAS method is sensitive to rigid materials when strong dipolar interactions in the system efficiently enhance the polarization transfer from protons to nearby carbons, thus enhancing the intensities of carbon resonances. On the other hand, the SPE/MAS method is sensitive to mobile components when a repetition time as short as 2 s is used. For WP materials (Fig. 5), the rigid component observed by the CP/MAS method was assigned to proteins with the C=O at 174 ppm, the C- α , C- β and C- γ at 54, and 30–15 ppm. The minor resonances at 157, 138, 129 and 116 ppm were due to Arg, Tyr and Phe.^{48–51} The resonances of residual starch were also obtained in the CP/MAS spectra of the WG materials at 103, 83 and 74 ppm (C-1, C-4 and C-2,3, and 5 of starch), while the C-6 could overlap with those of proteins at 64 ppm (Fig. 6). Lipid was the major mobile component observed in the SPE/MAS spectra for both the WP and WG materials in conjunction with plasticized proteins. Note that mobile starch signals were also observed in the SPE/MAS spectra for WG materials (Fig. 6). These results are similar to those obtained for other plasticized WP or WG materials.^{34–36,46,47} Bearing in mind that only 5 wt % of lipid existed in either the WP or WG raw materials, the SPE/MAS spectra indicate only a small proportion of proteins and starch in the mobile phase. The majority of proteins and starch remain in the rigid phase of the materials as detected by the CP/MAS method. An enhanced resonance at 63 ppm was indeed observed in the SPE/MAS spectra for both the WP and WG systems when AF or AFTR was used, indicating the existence of mobile AF segments (signals at 63 ppm for the $-\text{CH}_2\text{OH}$) in the systems.

High-resolution solid-state NMR techniques also provide a possibility to measure relaxation times for each component in a multi-component system. As seen in Figure 6, the protein resonances at 174 ppm and those of residual starch at 103 and 74 ppm are not overlapping to each other in the CP/MAS spectra; therefore, the

NMR relaxation parameters observed from these resonances should reflect the behaviour of the protein and starch components, respectively, in the systems. The ^1H T_1 results not only provide the information of molecular motions of each component in the system, but also reflect the homo- or heterogeneity of the whole material on a scale of ca. 20–30 nm, which is the effective spin-diffusion length during the ^1H T_1 times.^{51–55}

^1H T_1 data of the protein component in WP system observed via the CP/MAS method are listed in Table 4. The decrease in T_1 data when AF or AFTR is present in the WP materials is consistent with the plasticization effect as observed for other plasticized wheat protein materials.^{8,12} The difference in ^1H T_1 among the WP samples using AF or AFTR was minimal when a similar amount of resin was used (WP-A2 and WP-B samples). For the WG materials (Table 5), the T_1 data for both protein and starch components were decreased when AF or AFTR was used. These data indicated that the plasticization effect was predominant in both WP and WG materials. However, the T_1 data of the starch component in WG were decreased more significantly than those of the protein component when AF or AFTR was used. Starch contains a high proportion of

Table 4
 ^1H T_1 (s) of the protein components in WP materials

Samples	^1H T_1 (s)
WP-0	0.55 ± 0.01
WP-A1	0.45 ± 0.01
WP-A2	0.40 ± 0.01
WP-A3	0.41 ± 0.01
WP-B1	0.39 ± 0.01
WP-B2	0.38 ± 0.01
WP-B3	0.39 ± 0.01

Table 5¹H *T*₁ (s) of the protein and residual starch components in WG materials

Samples	Protein	Starch
WG-0	0.58 ± 0.01	0.86 ± 0.01
WG-A1	0.48 ± 0.01	0.58 ± 0.01
WG-A2	0.47 ± 0.02	0.55 ± 0.02
WG-A3	0.53 ± 0.02	0.58 ± 0.02
WG-B1	0.51 ± 0.01	0.62 ± 0.02
WG-B2	0.48 ± 0.01	0.58 ± 0.02
WG-B3	0.49 ± 0.01	0.58 ± 0.02

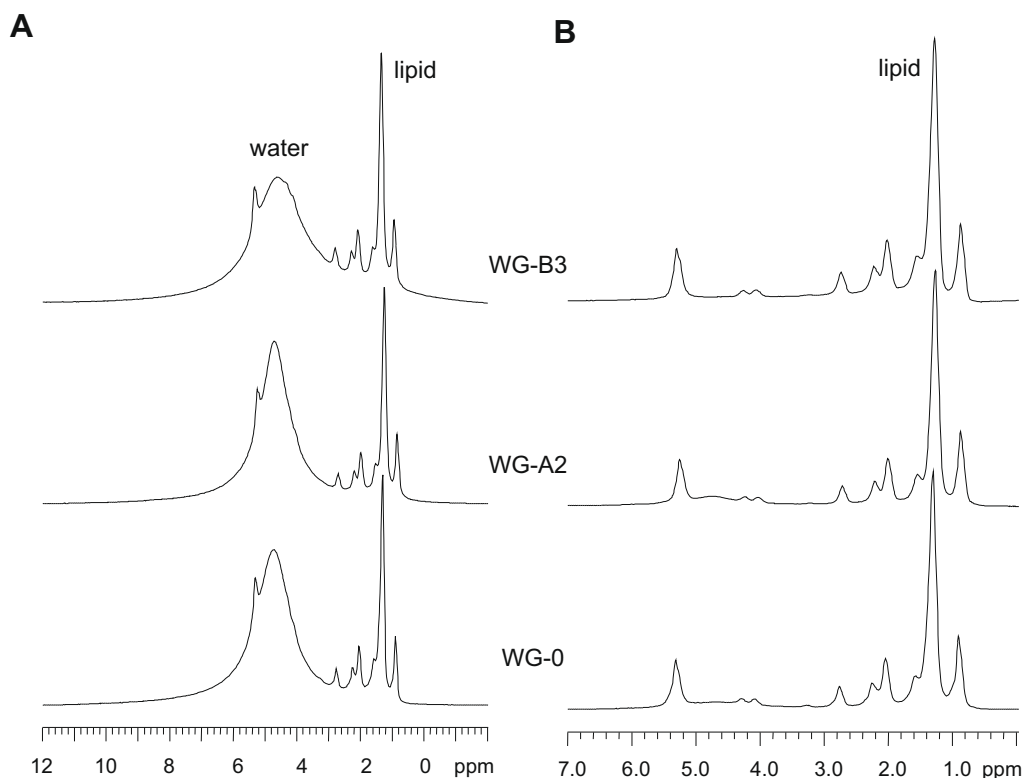
hydroxyl groups (three –OH groups in each repeat unit) that can act as interactive or reactive functional groups for either forming hydrogen bonding or undergoing condensation reactions with the AF or AFTR species. In contrast, the density of reactive or interactive functional groups in proteins (–NH₂, –OH, –SH, and so on) was much lower. It is possible that the residual starch (15% in WG) had associated with a higher ratio of AF or AFTR thus produced a more plasticized phase showing lower *T*_{g-start} data in the WG materials. Thus, the protein matrix of WG actually experienced a weaker plasticization effect than those experienced in the WP materials. Note that the *T*₁ data of the protein component in the WG systems were always higher than those in the WP materials. Such an effect in conjunction with the crosslinking resulted in a higher tensile strength and a lower elongation for the WG materials. The use of tannin further enhanced the tensile strength, implying its stronger reactivity with the protein matrix in the WG systems; however, this requires further chemistry studies. The difference in ¹H *T*₁ value observed for different components in the WG materials also suggests that the systems were heterogeneous on a scale of 20–30 nm, and the spin-diffusion effect did not average out the relaxation process of the whole WG materials.

The mobility of the lipid and moisture in the WP and WG materials was examined by ¹H *T*₂ measurement via ¹H MAS spectra

using the same method as we reported previously for other plasticized WG materials.^{12,18,34,46,47} Figure 7 shows the ¹H spectra of WG-0, WG-A2 and WG-B3 observed by CPMG pulse sequence with a short (0.1 ms) or a long (3 ms) *τ* times at which the *n*th echo appeared. The peaks at 0.9, 1.3, 2.0, 2.7 and 5.3 ppm were all assigned to lipid resonances, while the broad peak at 4.6–4.8 ppm was due to moisture in the materials.⁵⁶ A minor number of resonances of the plasticized proteins and AF (if it exists) might be overlapping with the broad/strong water peak. As the *τ* time increased, the intensity of the water peak at 4.6–4.8 ppm decayed much faster than those of lipid resonances, and only lipid signals were detected at *τ* = 3 ms, indicating that the lipid was still more mobile than water molecules in the system. The ¹H *T*₂ data observed by the CPMG pulse sequence (Table 6) suggest that the lipid did not take part in the interaction or reactions with AF or AFTR because its *T*₂ data remained at a level similar to that in WP-0 or WG-0. The *T*₂ data of the moisture partially reflected the mobility of the material

Table 6¹H *T*₂ (ms) of the moisture and lipid in WP or WG materials

Samples	Moisture (4.6 ppm)	Lipid (1.3 ppm)
WP-0	0.23 ± 0.01	27.7 ± 2.1
WP-A1	0.80 ± 0.01	26.0 ± 2.1
WP-A2	0.85 ± 0.02	25.7 ± 1.9
WP-A3	0.97 ± 0.02	26.4 ± 1.6
WP-B1	0.71 ± 0.02	30.3 ± 2.1
WP-B2	0.70 ± 0.02	29.7 ± 2.2
WP-B3	0.67 ± 0.01	28.5 ± 2.3
WG-0	0.23 ± 0.01	22.5 ± 1.4
WG-A1	0.62 ± 0.01	21.1 ± 1.5
WG-A2	0.66 ± 0.02	22.6 ± 1.6
WG-A3	0.61 ± 0.01	23.4 ± 1.6
WG-B1	0.47 ± 0.02	22.4 ± 2.0
WG-B2	0.45 ± 0.02	21.1 ± 2.1
WG-B3	0.40 ± 0.01	22.2 ± 1.9

**Figure 7.** ¹H MAS NMR spectra of WG-0, WG-A2 and WG-B3 samples obtained by CPMG pulse sequence with *τ* delay of (A) 0.1 ms and (B) 3 ms.

matrix as most of these small water molecules were associated intimately with protein or starch macromolecules through hydrogen bonding when the moisture content was around 10–11%. The increase in T_2 of the moisture in the materials containing AF or AFTR indicates the mobility increase of the polymer matrix, which is consistent with the predominant plasticization effect, and the lower T_2 values in the WG system (than those of WP samples) provided additional evidence for the weaker plasticization effect on the WG matrix as detected in ^1H T_1 observation, where proteins were the major component in the material matrix.

4. Conclusions

Mobile AF resin containing both interactive and reactive functional groups was able to act as an efficient plasticizer for wheat proteins to produce renewable and biodegradable plastics with sufficient flexibility. The covalent bonds formed between AF and the protein matrix via condensation reactions under thermal processing conditions resulted in a sufficient retention of the water-soluble resin in the materials under wet conditions. The low cross-link density formed through the polymer matrix was ideal for achieving the plasticization effect for the materials, and the mechanical properties were also enhanced as an additional benefit due to formation of such crosslinked networks. The tensile strength could be further enhanced when using natural tannin in conjunction with AF resin in the systems because of the formation of crosslinking segments involving rigid aromatic structures derived from tannin. Different components in the WP or WG resins (e.g., proteins, residual starch and lipids) displayed different capabilities in interaction and reaction with the AF additives, which resulted in different performance properties when the ratio of these components varied in the materials. WG systems containing 15% of residual starch displayed a higher tensile strength and a lower elongation as compared to the WP systems. The application of AF/AFTR additives provided a feasible methodology to thermally process wheat protein-based natural polymer materials with improved mechanical performance especially under wet conditions.

References

- Ali, Y.; Ghorpade, V. M.; Hanna, M. A. *Ind. Crops Prod.* **1997**, *6*, 177–184.
- John, J.; Tang, J.; Bhattacharya, M. *Polymer* **1998**, *39*, 2883–2895.
- Redl, A.; Morel, M.; Bonicel, J.; Vergnes, B. *Cereal Chem.* **1999**, *76*, 361–370.
- Micard, V.; Morel, M.-H.; Bonicel, J.; Guilbert, S. *Polymer* **2001**, *42*, 477–485.
- Gallstedt, M.; Mattozzi, A.; Johansson, E.; Hedenqvist, M. S. *Biomacromolecules* **2004**, *5*, 2020–2028.
- Zhang, X.; Burgar, I.; Loubakos, E.; Beh, H. *Polymer* **2004**, *45*, 3305–3312.
- Zhang, X.; Do, M.; Loubakos, E. *Polym. Prepr.* **2005**, *46*, 321–322.
- Zhang, X.; Burgar, I.; Do, M.; Loubakos, E. *Biomacromolecules* **2005**, *6*, 1661–1671.
- Pouplin, M.; Redl, A.; Gontard, N. *J. Agric. Food Chem.* **1999**, *47*, 538–543.
- Redl, A.; Morel, M.; Bonicel, J.; Guilbert, S.; Vergnes, B. *Rheol. Acta* **1999**, *38*, 311–320.
- Zhang, X.; Burgar, I.; Do, M.; Loubakos, E.; Beh, H. *Polym. Prepr.* **2003**, *44*, 402–403.
- Zhang, X.; Do, M.; Hoobin, P.; Burgar, I. *Polymer* **2006**, *47*, 5888–5896.
- Irissin-Mangata, J.; Bauduin, G.; Boutevin, B.; Gontard, N. *Eur. Polym. J.* **2001**, *37*, 1533–1541.
- Pommet, M.; Redl, A.; Morel, M. H.; Guilbert, S. *Polymer* **2003**, *44*, 115–122.
- Pommet, M.; Redl, A.; Guilbert, S.; Morel, M.-M. *J. Cereal Sci.* **2005**, *42*, 81–91.
- Micard, V.; Belamri, R.; Morel, M.-H.; Guilbert, S. *G. J. Agric. Food Chem.* **2000**, *48*, 2948–2953.
- Hernandez-Munoz, P.; Villalobos, R.; Chiralt, A. *Food Hydrocolloids* **2004**, *18*, 403–411.
- Zhang, X.; Hoobin, P.; Burgar, I.; Do, M. *J. Agric. Food Chem.* **2006**, *54*, 9858–9865.
- Orliac, O.; Rouilly, A.; Silvestre, F.; Rigal, L. *Polymer* **2002**, *43*, 5417–5425.
- Ghorpade, V. M.; Li, H.; Gennadios, A.; Hanna, M. A. *Trans. ASAE* **1995**, *38*, 1805–1808.
- Park, S. K.; Bae, D. H.; Rhee, K. C. *J. Am. Oil Chem. Soc.* **2000**, *77*, 879–883.
- Rhim, J. W.; Gennadios, A.; Handa, A.; Weller, C. L.; Hanna, M. A. *J. Agric. Food Chem.* **2000**, *48*, 4937–4941.
- Lieberman, E. R.; Guilbert, S. G. *J. Polym. Sci. Symp.* **1973**, *41*, 33–43.
- Parris, N.; Coffin, D. R. *J. Agric. Food Chem.* **1997**, *45*, 1596–1599.
- Galiati, G.; di Gioia, L.; Guilbert, S.; Cuq, B. *J. Dairy Sci.* **1998**, *81*, 3123–3130.
- Marquie, C.; Aymard, C.; Cuq, J. L.; Guilbert, S. *J. Agric. Food Chem.* **1995**, *43*, 2762–2767.
- Marquie, C. *J. Agric. Food Chem.* **2001**, *49*, 4676–4681.
- Happich, W. F.; Windus, W.; Naghschi, J. *Text. Res. J.* **1965**, *35*, 850–852.
- Di Monica, G.; Marzona, M. *Text. Res. J.* **1971**, *41*, 701–705.
- Tropini, V.; Lens, J.-P.; Mulder, W. J.; Silvestre, F. *Ind. Crops Prod.* **2003**, *20*, 281–289.
- Kuijpers, A. J.; Engbers, G. H. M.; Feijen, J.; de Smedt, S. C.; Meyvis, T. K. L.; Demeester, J.; Krijgsveld, J.; Zaat, S. A. J.; Dankert, J. *Macromolecules* **1999**, *32*, 3325–3333.
- Van Wachem, P. B.; Zeeman, R.; Dijkstra, P. J.; Feijen, J.; Hendriks, M.; Cahalan, P. T.; van Luyn, M. J. A. *J. Biomed. Mater. Res.* **1999**, *47*, 270–277.
- Sung, H.-W.; Huang, D.-M.; Chang, W.-H.; Huang, R.-N.; Hsu, J.-C. *J. Biomed. Mater. Res.* **1999**, *46*, 520–530.
- Zhang, X.; Do, M.; Bilyk, A. *Biomacromolecules* **2007**, *8*, 1881–1889.
- Kurniawan, L.; Qiao, G. G.; Zhang, X. *Biomacromolecules* **2007**, *8*, 2909–2915.
- Kurniawan, L.; Qiao, G. G.; Zhang, X. *Macromol. Biosci.* **2009**, *9*, 93–101.
- Albrecht, N. G.; Foran, M. T. European Patent EP0672693, June 2001.
- Swiezowski, F. J.; Bilmers, R. L.; Mwonya, P. B.; Seaman, G. W. U.S. Patent 6,648,955, October, 2000.
- Garcia, R.; Pizzi, A. *J. Appl. Polym. Sci.* **1998**, *70*, 1093–1109.
- Simon, C.; Pizzi, A. *J. Appl. Polym. Sci.* **2002**, *88*, 1889–1903.
- Bisanda, E. T. N.; Ogola, W. O.; Tesha, J. V. *Cem. Compos.* **2003**, *25*, 593–598.
- Li, K.; Geng, X.; Simonsen, J.; Karchesy, J. *Int. J. Adhes. Adhes.* **2004**, *24*, 327–333.
- Kato, A.; Tanaka, A.; Lee, Y.; Matsudomi, N.; Kobayashi, K. *J. Agric. Food Chem.* **1987**, *35*, 285–288.
- Gennadios, A.; Brandenburg, A. H.; Weller, C. L.; Testin, R. F. *J. Agric. Food Chem.* **1993**, *41*, 1835–1839.
- Ayserlioglu, B. S.; Stevels, W. M.; Mulder, W. J.; Akkas, N. *Starch/Stärke* **2001**, *53*, 381–386.
- Zhang, X.; Hoobin, P.; Burgar, I.; Do, M. *Biomacromolecules* **2006**, *7*, 3466–3473.
- Zhang, X.; Do, M.; Dean, K.; Hoobin, P.; Burgar, I. *Biomacromolecules* **2007**, *8*, 345–353.
- Belton, P. S.; Duce, S.; Colquhoun, I. J.; Tatham, A. S. *Magn. Reson. Chem.* **1988**, *26*, 245–251.
- Belton, P. S.; Colquhoun, I. J.; Grant, A.; Weliner, N.; Field, J. M.; Shewry, P. R.; Tatham, A. S. *Int. J. Biol. Macromol.* **1995**, *17*, 74–80.
- Yoshimizu, H.; Ando, I. *Macromolecules* **1990**, *23*, 2908–2912.
- Havenes, J. R.; VanderHart, D. L. *Macromolecules* **1985**, *18*, 1663–1676.
- Dickinson, L. C.; Yang, H.; Chu, C.-W.; Stein, R. S.; Chien, J. C. W. *Macromolecules* **1987**, *20*, 1757–1760.
- Zhang, X.; Takegoshi, K.; Hikichi, K. *Macromolecules* **1991**, *24*, 5756–5762.
- Zhang, X.; Takegoshi, K.; Hikichi, K. *Macromolecules* **1993**, *26*, 2198–2201.
- Zhang, X.; Solomon, D. H. *Macromolecules* **1994**, *27*, 4919–4926.
- Calucci, L.; Forte, C.; Galleschi, L.; Geppi, M.; Ghiringhelli, S. *Int. J. Biol. Macromol.* **2003**, *32*, 179–189.